Proteomic Response of Sugar Beet Monosomic Addition Line M14 Guard Cells to Salt Stress

Jialin Zhang
Ministry of Education, Heilongjiang University
Xin Tao
Ministry of Education, Heilongjiang University
Shuang Wang
Ministry of Education, Heilongjiang University
Jinna Li
Ministry of Education, Heilongjiang University
He Liu
Ministry of Education, Heilongjiang University
Sixue Chen
University of Florida
Bing Yu
Ministry of Education, Heilongjiang University
Chunquan Ma
Ministry of Education, Heilongjiang University
Haiying Li (lvzh3000@sina.com)
Ministry of Education, Heilongjiang University

Research Article

Keywords: proteomics, guard cells, stomata, salt stress, sugar beet M14, molecular mechanisms

Posted Date: March 8th, 2022

DOI: https://doi.org/10.21203/rs.3.rs-1025655/v1

Abstract

Background

Soil salinity is one of the most detrimental abiotic stresses that limit crop production and threaten global food security. The responsiveness of stomatal guard cells to various stimuli is important for plants to balance transpirational water loss and carbon dioxide (CO_2) intake for photosynthesis. It is important to identify differences in proteomic changes under salt stress and to understand the mechanisms underlying salt stress-induced stomatal movement in sugar beet guard cells through proteomic analysis.

Results

In this study, we observed stomatal closure and changes in ascorbate peroxidase activities during short-term salt stress treatment of sugar beet monosomic addition line M14. We analyzed proteomic changes in guard cells in response to the salt stress using an iTRAQ-based quantitative proteomic approach. A total of 142 proteins were differentially changed in guard cells by the salt stress treatment. They include several ribosomal proteins, metabolic enzymes and photosystem-related proteins. Gene ontology (GO) annotation of the differentially abundant proteins highlights most of the proteins are related to binding activity, response to stimuli, and glutathione metabolism, phenylpropanoid biosynthesis and carbon fixation pathways. Many of the proteins were targeted to the chloroplast, nucleus and cell wall. They may play an important role in the process of stomata closure. In addition, several antioxidant enzymes (e.g., peroxidase, ascorbate peroxidase and dehydroascorbate reductase) involved in the regulation of ROS homeostasis were identified. Transcriptional levels of 16 differential proteins involved in stress responses did not correlate well with the protein levels, indicating different regulatory mechanisms in guard cells.

Conclusions

The proteomics results have revealed interesting mechanisms underlying the sugar beet guard cell response to salt stress, which have not been reported before. The knowledge may facilitate molecular breeding and/or engineering efforts toward enhancing crop stress tolerance while not compromising yield.

Background

Plant leaves are composed of different types of cells, such as mesophyll, epidermal and guard cells (GCs). Each type of cells may play different roles in plant growth, development and response to environmental stimuli. Guard cells are specialized paired cells that border the pores on leaf surfaces called stomata [1]. Closing and opening of stomata controls the balance of water transpiration and CO_2 intake for photosynthesis [2]. Plants adjust their stomatal aperture by changing turgor pressure to adapt to abiotic and biotic stresses, such as salt stress. With the intensification of climate change, soil

salinization has become a global problem [3]. It negatively impacts plant growth and development, and represents a destructive threat to global agricultural production [4].

It is well-known that salt stress induces a dramatic increase in abscisic acid (ABA) biosynthesis, reactive oxygen species (ROS) production and Ca^{2+} oscillation in the cytosol [5, 6]. Each of these changes may lead to stomatal closure, thus imposes yield penalties to crops [7]. Most crops are sensitive to salinity, even under moderate soil salinity. However, there is a special group of plants, called halophilic plant, which can deal with high root zone salinity [8]. Moreover, halophilic not only survive, but also thrive under the saline conditions. Therefore, a better understanding of the molecular mechanisms by which halophilic regulate their stomatal movement is important for us to improve plant salt tolerance and enhance crop production.

Sugar beet monosomic addition line M14 (*BvM14* line) was obtained from the intercross between *Beta vulgaris* L. and *B. corolliflora* Zoss. It contains the *Beta vulgaris* L. genome with the addition of chromosome 9 of *B. corolliflora* Zoss and has the trait for apomixes [9]. In addition, our previous studies have shown that *BvM14* line can tolerate 500 mM NaCl treatment and exhibits strong salt tolerance [10]. Thus, BvM14 is an ideal halophilic plant for studying the molecular mechanism of stomatal movement in response to salt stress [11–13]. Most studies on stomatal guard cell signaling were done with stress treatments to the leaf or isolated guard cells. For example, Zhu *et al*. identified 65 and 118 potential redox proteins in isolated *Brassica napus* guard cells treated directly with ABA and methyljasmonate (MeJA), respectively [14]. This was the first time that a protein redox regulatory mechanism was discovered in guard cell ABA and MeJA signal transduction. Zhang *et al*. used cysTMT tagging technology to identify 80 thioredoxin target proteins in *B. napus* guard cells. These redox proteins play important roles in photosynthesis, stress response and cell signaling pathways [15]. While an extensive effort has been made in genetic, physiological and proteomic studies of guard cell responses in leaves or isolated cells, little research has been done to investigate guard cell molecular changes in response to short-term salt stresses applied to the roots, a situation that plants experience frequently in natural conditions.

In this work, we applied an iTRAQ LC-MS/MS technology for quantitative proteomic analysis of guard cell proteins in the *BvM14* line in response to short-term salt treatment to the roots. A number of differentially abundant proteins were identified and quantified, including 90 and 75 differentially abundant proteins (DAPs) under 200 mM and 400 mM NaCl treatment, respectively. Gene ontology (GO) annotation of the DAPs highlights most are relevant to binding activity, and are involved in glutathione metabolism, phenylpropanoid biosynthesis and carbon fixation pathways. Subcellular localization analysis revealed most of the DAPs were targeted to the chloroplast, nucleus and cell wall. In addition, transcriptional levels of 16 DAPs were determined using real-time PCR. Based on our results, we proposed a model of molecular networks underlying the stomatal movement in the *BvM14* response to short-term salt stress.

Materials And Methods

Plant Materials and NaCl Treatment

Sugar Beet Monosomic Addition Line M14 (Chromosome 9 monosomic addition line of *Beta corolliflora* Zoss. in *Beta vulgaris* L., VV+C9, 2n=18+1, CN1263695A) were grown in a greenhouse of Heilongjiang University. The *BvM14* line seeds were sterilize with 0.1% (w/w) mercurial chloride and 0.2% (w/w) thiram, and then sown in vermiculite for germination. After 10 days, the seedlings were transferred to hydroponic containers containing the Hoagland solution [16]. Seedlings were grown in a growth chamber with a 13h light/11h dark cycle, 25/20 ^{o}C day/night temperature, 450 μmol m^{-2} s^{-1} light intensity and a relative humidity of 70%. Five-week-old *BvM14* line were divided into three groups, i.e., control group (without NaCl), treatment groups (200 mM or 400 mM NaCl) for 10, 20, 30, 40, 50 and 60 min. The NaCl concentrations were chosen according to our previous report showing that the *BvM14* line can tolerate up to 500 mM NaCl [10]. Three biological replicates were conducted for all the experiments.

Large-Scale Preparation of Stomatal Guard Cells

Two methods were commonly used for obtaining enriched guard cells, i.e., transparent tape-peel method and the blender pulverization method. We performed both, and optimized the latter for preparing stomatal guard cells from *BvM14* line. Briefly, the main and secondary veins of leaves were removed with a scalpel. Then the leaves were blended for 30 seconds each time for a total of three times in a blender to remove the mesophyll cells. Epidermal peels were collected on a 100 μm nylon mesh and washed thoroughly with tap water to remove any broken cells and small dark green tissue fragments were removed using clean forceps. The peels were transferred to a beaker containing 200 mL digesting enzyme mixture and digested for 20 minutes. The digesting enzyme mixture contained 4.2% cellulase R-10, 015% macerozyme R-10 and 0.2% pectolyase Y-23. Enriched stomata on digested peels were collected on the 100 μm nylon mesh and washed thoroughly with 750 mL basic solution (0.55M sorbitol; 0.5 mM $CaCl_2$; 0.5 mM $MgCl_2$; 0.5 mM ascorbic acid; 10μM; KH_2PO_4; 5 mM MES; Add Tric-HCl (pH=8.0) to adjust the pH of solution to 5.5). Samples were used fresh for activity assays or snap-frozen in liquid nitrogen and were kept in -80℃ freezer until used for protein extraction.

Stomatal Movement and Ascorbate Peroxidase (APX) Activity Assay

The epidermis of the leaves of *BvM14* line was removed and fixed in a freshly prepared Carnoy fixative solution (3 parts 100% ethanol : 1 part acetic acid, v/v) for 45 seconds. After fixation, the epidermis was dehydrated in 70% ethanol and then in 100% ethanol, each for 5 minutes. Laser Scanning Confocal Microscope (Olympuj, Japan) was used for imaging and stomatal aperture was measured by image J software.

For APX assay, 2 g of leaves were used to enrich the guard cells as one replicate. Three replicate samples were collected. The enriched sample was homogenized in a mortar and pestle while adding 50 mM phosphate buffer solution (pH: 7.8). After centrifugation at 12000 rpm, 4 ^{o}C, the supernatant was used for

APX activity assay. Three replicates were prepared for each sample. The APX activity was assayed by measuring the absorbance value at 290 nm using a spectrophotometer. A total of 2 mL reaction mixture contained 1.65 mL phosphate buffer, 100 µL 5 mM ascorbic acid (ASA), 100 µL 20 mM H_2O_2 and 150 µL enzyme extract. APX activity was defined as the amount of ascorbic acid reduction per minute.

Protein Extraction

Protein extraction from the *BvM14* line guard cells was performed according to a phenol extraction method [17]. Briefly, the enriched guard cells were ground into a fine powder in liquid nitrogen and suspended in 3.75 mL Tris saturated phenol (pH 8.8) and 2.5 mL phenol extraction buffer (25 mM TEAB, 10 mM EDTA, 200 mM DTT, 200 mM PMSF, and 900 mM sucrose). The mixture was agitated for 2 hours at room temperature and then centrifuged at 10000×g for 10 min, at 10 ^{o}C. The upper phenol phase was transferred to a new tube. The bottom phase was extracted with phenol again and then centrifuged under the same condition. The upper phenol phase was transferred to the same tube. Proteins were precipitated from the phenol phase by the addition of five volumes of 0.1 M ammonium acetate in methanol at -20 ^{o}C overnight. Precipitated proteins were centrifuged at 10000×g 4 ^{o}C for 20 min and then discard the supernatant. The precipitate was washed twice with 0.1 M ammonium acetate in methanol, then twice with 80% cold acetone and once with 100% cold acetone. Finally, the precipitate was solubilized in urea buffer (6 M urea, 0.5% SDS, 25 mM TEAB, 1 mL Triton X-100), and the protein concentration was determined with a BCA kit [12].

Trypsin Digestion and Desalting

Guard cell protein extracts were reduced with 10 mM DTT for 1 h, alkylated with 55 mM iodoacetamide in darkness at room temperature for 1 h, followed by digestion with trypsin (Sequencing grade, Promega, Madison, WI, USA) at a ratio of 1:50 (w/w) overnight at 37 ^{o}C [18]. Trifluoroacetic acid (TFA) was added to stop the reaction at a final concentration of 0.1%. The tryptic digests were desalted by solid phase extraction (SPE). The SPE is C18-based and the peptides were eluted with 80% acetonitrile/0.1% formic acid [13].

iTRAQ Labeling and Strong Cation Exchange (SCX) Fractionation

Peptides derived from 50 µg protein digests were reconstituted in 25 µL 0.5 M TEAB solution. Labeling with the iTRAQ 8-plex reagents was conducted according to the manufacturer's instructions (AB Sciex Inc., Framingham, MA, USA). The entire set of samples was divided into two groups, in one group the control replicates were labeled with iTRAQ tags 114, 116,118 and 121; the 200 mM NaCl replicates with tags 113, 115, 117 and 119. In the other group the control replicates were labeled with iTRAQ tags 114,

116, 118 and 121; the 400 mM NaCl replicates with tags 113, 115, 117 and 119. The labeled peptide samples from each group were mixed and lyophilized. The samples were resolubilized in strong cation exchange (SCX) solvent A (25% v/v acetonitrile, 10 mM ammonium formate, and 0.1% v/v formic acid, pH 2.8). The peptides were fractionated using an Agilent high performance liquid chromatograph (HPLC) 1260 with a SCX column (PolySULFOETHYL A, 100 × 2.1 mm, 5 µM, 300 Å). Peptides were eluted with a linear gradient of 0-20% solvent B (25% v/v acetonitrile and 500 mM ammonium formate, pH 6.8) over 80 min, followed by ramping up to 100% solvent B in 5 min [11, 19, 20]. Peptide absorbance at 280 nm was monitored, and 32 fractions were collected. Each fraction was desalted ZipTips according to manufacturer's manual (MilliporeSigma, St. Louis, MO, USA), and then lyophilization to dryness.

LC-MS/MS of the SCX fractions and Data Analysis

Each peptide sample was solubilized in reverse phase solvent A (0.1% formic acid, v/v), and loaded onto a liquid chromatography tandem mass spectrometry (LC-MS/MS) system. The experiment was performed on an Easy-nLC 1000 system (Thermo Fisher Scientific, Bremen, Germary), connected to a hybrid quadrupole orbitrap mass spectrometer. The peptides were loaded onto an Acclaim C18 PepMap 100 pre-column (20 mm × 75 µm; 3 µm) and separated on a C18 PepMap RSLC analytical column (500 mm × 75µm; 2 µm) at a flow rate at 300 nl/min during a linear gradient from the solvent A to 30% solvent B (0.1% formic acid and 99.9% acetonitrile, v/v) in 110 min, and to 98% solvent B for additional 7 min [11]. Full MS scans were acquired in the Q-Exactive Orbitrap mass analyzer over m/z 400–2000 range with resolution 70,000 at 200 m/z. The top ten most intense peaks with charge stated more than 2 were isolated with a 1.3 m/z isolation window and fragmented in the high energy collision cell using a normalized collision energy of 28%. The first mass to include for the MS/MS was 110. The maximum ion injection time for the survey scan and the MS/MS scans were 250 ms, and the ion target values were set to 3e6 and 1e6, respectively. The selected sequenced ions were dynamically excluded for 60 sec.

The MS/MS spectra were searched against the *B. vulgaris* database (52,749 entries) using Proteome Discoverer 2.1 (Thermo Fisher Scientific, Bremen, Germany). Trypsin was specified as the enzyme, and two missed cleavages were permitted; Fragment mass tolerance was 0.02 Da and peptide tolerance mass was 10 ppm; iTRAQ8plex (N-term) and iTRAQ8plex (K) were fixed modifications. To be determined as being significantly differentially accumulated, a protein should be quantified in at least two out of three biological replicates with a corrected p-value of <0.05 and a fold change <0.8 or >1.2. All the proteins were blasted against UniProt (http://www.ebi.uniprot.org) for functional annotations and the GI numbers of the homologous proteins in UniProt were used to indicate annotations. Four subcellular location databases of LocTree3, ngLOC, Plant-mPLoc and soft berry were used to perform subcellular location of differentially abundant proteins, and the locations that appear at least twice were selected as the final subcellular location result. GO enriched was done using an online tool AgriGO (http://bioinfo.cau.edu.cn/agriGO). All the proteomics data and search results have been deposited to the ProteomeXchange Consortium via the PRIDE [21] partner repository with the dataset identifier PXD026328 (Username: reviewer_pxd026328@ebi.ac.uk Password: IWQcnkJe).

Quantitative RT-PCR Analysis

Total RNA was isolated from frozen samples using a TRIZOL reagent (Invitrogen) and the synthesis of the first strand of cDNA was carried out using a reverse transcription kit (Takara, Shiga, Japan). Gene specific primers were designed using online Primer3 Plus according to a previously published procedure[22]. Quantitative RT-PCR system was performed in a 10 μL volume containing 5 μL of Power UpTM SYBRTM Green Master (Applied Biosystems, Vernon, CA, USA), 1 μL cDNA, 0.4 μL of each gene-specific primer, and 3.2 μL double distilled H_2O. The PCR conditions were as follows: 95 °C for 2 min; 95 °C for 15 s, 60 °C for 1 min, 40 cycles. The expression levels were determined with the $2^{-\Delta\Delta CT}$ method [23].

Results

Development of Sugar beet Guard Cell Enrichment Protocol

Since our experiment starts with salt stress treatment of the plant roots and then focuses on analyzing guard cells on the leaves, we need to use a fast and efficient guard cell enrichment method. The enrichment process of guard cells is divided into two steps: isolation of epidermal fragments and digestion of epidermal fragments. There are two commonly used methods for obtaining the epidermal fragments, the transparent tape-peel method [24] and the blender pulverization method [1, 25]. We first obtained the epidermal fragments of *BvM14* line through these two methods (Figure 1A, 1B). The obtained epidermal fragments were then treated by 2.1% cellulase R-10, 0.075% macerozyme R-10 (Figure 1C, 1D). We observed that the guard cells obtained by the tape-peel method has a large amount of mesophyll cells contamination even after the enzyme treatment. In contrast, the guard cells obtained by the blender method are less contaminated, but this method requires enzymatic digestion for six hours to achieve high quality. This long processing time may cause artificial molecular changes, which can affect downstream proteomic analyses [26]. Therefore, we chose to use the blender pulverization method to obtain epidermal peers and adjusted the type and concentration of enzymes to shorten the enzymatic hydrolysis time to 20 minutes. Finally, we found that the guard cells could be rapidly enriched by using 4.2% cellulase R-10, 0.075% macerozyme R-10 and 0.2% pectolyase Y-23 [1, 2, 27]. As shown in the Figure 1D, the pavement cells were digested away, and stomatal guard cells were of high quality. Purity was further confirmed by a purity assay of the guard cell samples using Real-Time PCR for a guard cell-specific transcript *H^+-ATPase* (*AHA1*). As shown in Figure S1A, the transcript levels of sugar beet *AHA1* (specifically expressed in guard cells) was 70 times higher in the enriched guard cells than in leaves, indicating little contamination of guard cell samples from mesophyll cells. In addition, high level distribution of *AHA1* expression in different cells of leaves from ePlant (https://bar.utoronto.ca/ePlant/) has further proved that *AHA1* is a guard cell-specific gene (Figure S1B). Our method greatly shortens the enrichment time of guard cells and reduces contamination from other types of cells, such as mesophyll cells and epidermal pavement cells. It is suitable for guard cell proteomics experiments.

Stomatal Movement and Activity of APX in Response to Salt Stress

Previous studies have shown that when plants are exposed to salt stress, stomata may close transiently, but over the long term adaptation, plants will not compromise diurnal stomatal movements in response to the day-night cycle [28, 29]. To investigate responses of stomatal movement to short-term salt stress, we measured how salt stress affected *BvM14* line stomatal aperture at seven different time points (0, 10, 20, 30, 40, 50, 60 min), and selected the time points when stomatal aperture became the smallest for proteomic analysis. In order to determine the most suitable method for stomatal movement assays. We first referred to a method in a previous study for measuring the stomatal aperture of *Triticum aestivum* [30]. We spread clear nail varnish on the abaxial side of the selected leaves. Then peeled the dried nail polish molds off with a tweezer. The slides were visualized under a laser scanning confocal microscope (Olympuj, Japan) (Figure S2A). This method clearly reflects the size of the stomata, but in subsequent experiments we found that this method has poor repeatability and a lot of damage to the leaves, thus is not suitable for our experiments. After consultation and literature searching, we tested a method that involves fixation of the leaves [31]. This method turned out to be reproducible, but it took a long time. (Figure S2B). It still did not meet the need of our experiment. Finally, through our own optimization, we were able to capture the changes of stomatal apertures in a short period of time (Figure S2C). Briefly, after tearing off the abaxial epidermal peels from the sugarbeet M14 leaves, we fixed the leaves in a freshly prepared Carnoy fixative solution (3 parts 100% ethanol : 1 part acetic acid, v/v) for 45 seconds, and then dried and viewed under microscope. Using this method, we observed that the stomatal aperture reached the lowest level under 200 mM and 400 mM NaCl treatments at 20 and 30 minutes, respectively (Figure 2A). Since the closing of the stomata is caused by the perception of ABA and H_2O_2 signals triggered by salt stress, the changes in protein levels may precede the changes in the stomatal aperture. Thus, in order to accurately determine the optimal time points for proteomics of guard cell response to salt stress, we measured APX activities, which can reduce H_2O_2 contents in plant. As shown in Figure 2B, under 200 and 400 mM NaCl treatments, the APX activities reached the highest levels at 10 min and 20 min, respectively. The time for APX activities to reach its peak is 10 minutes earlier than the time for stomatal aperture to reach its smallest level, regardless of whether the plants were treated with 200 or 400 mM NaCl. Therefore, we used the APX assay results to determine the time points for the proteomics experiments.

iTRAQ Analysis of Differentially Abundant Proteins (DAPs)

To examine the proteomic changes in guard cells in response to the salt stress, three biological replicates were analyzed for each control and treatment. Under the 200 mM NaCl treatment, 12,672 peptide spectrum matches (PSMs) and 1796 proteins were identified against the Sugar beet database, of which 1069 of the proteins had at least two unique peptides. Under the 400 mM NaCl treatment, 13,170 PSMs and 1609 proteins were identified, where 989 of the proteins had at least two unique peptides. The

peptide number distribution of proteins indicates that approximately 60% of identified proteins contained more than two unique peptides (Figure S3). The distribution of protein mass is mostly in the range of 10 to 60 kDa (Figure S4).

To identify proteins significantly affected by salt stress. Protein with at least two unique peptides were used to screen for DAPs with a *p*-value < 0.05 and a fold-change > 1.2. Under the 200 mM NaCl treatment, 80 DAPs were identified, of which 40 were increased and 40 were decreased. Under the 400 mM NaCl treatment, 72 DAPs were identified, including 17 increased and 55 decreased compared to control samples. The DAPs with fold-changes > 2 were marked in the volcano plot (Figure 3A and 3B). At the level of individual proteins, we found that a non-specific lipid-transfer protein (W6JNH5) was increased by 3- and 2-fold under 200 mM and 400 mM NaCl, respectively. Non-specific lipid-transfer protein (nsLTP) has been found to modulate plant tolerance to salt, drought, cold stresses, as well as defense against bacterial and fungal pathogens [32-34]. Our results indicate that nsLTP may play a vital role in the process of guard cells against salt stress. The overlap between the DAPs is shown in Figure 3C. In the two different salt concentration groups, five proteins were observed to be regulated in the same trend (both decreased or both increased in two groups). The other DAPs did not show this kind of concerted changes. The result indicates some shared components between the two salt treatment groups had conserved responses to the short-term salt stress treatments. A detailed description of DAPs is shown in Supplemental Tables S1 and S2.

The global expression of DAPs was further estimated using hierarchical clustering analysis. The results were displayed in the heat map (Figure 4A and 4B). The cluster analysis showed that the proteins of both groups were similar in distance and preferentially sorted together, indicating that the sample repeatability of the control groups and the treatment groups was good. At the same time, results also showed that the DAPs were well-distinguished and selected. Overall, the heat map provided a better visualization of the proteomic changes between control groups and treatment groups.

Bioinformatic Analysis of the DAPs

Bioinformatic analysis of the DAPs can provide an in-depth understanding of the proteomics result [35]. To reveal potential molecular mechanisms underlying the guard cell response to the salt stress, gene ontology (GO) functional classification of the DAPs was conducted based on the molecular function, cellular components and biological processes. We compared the GO classification of DAPs under 200 mM and 400 mM NaCl treatments. As shown in Figure 5A, both salt stress conditions showed similar patterns in molecular function, cellular components, and biological process. In the molecular function analysis, proteins with binding and structural constituent of ribosome were differentially expressed under the 200 mM NaCl and 400 mM NaCl treatments. These proteins include photosynthesis-related proteins (oxygen-evolving enhancer protein 2 and oxygen-evolving enhancer protein 3), which may play an important role in energy balance in response to the salt stress. In the cellular component, the proteins were mainly located in the plastid. Compared with the 200 mM NaCl result, the 400 mM NaCl treatment

had more proteins in the ribosome and cytosol. In the biological process, proteins were enriched in 36 processes, including response to stress, translation, catabolic process, carbohydrate metabolic process, etc., implying that severe salt stress induced DAPs in a larger number of biological processes. AgriGO functional enrichment results were consistent with those in Figure 5A. In the molecular function category, proteins with RNA binding and structural constituent of ribosome were enriched (Figure S5). In terms of cellular components, plastid, chloroplast part, cytoplasm and organelle part proteins were highly enriched (Figure S6). In biological processes, proteins involved in response to stress, response to abiotic stimulus and translation were significantly enriched (Figure S7).

To gain insights into the potential functions of the DAPs and their metabolic pathways, Kyoto Encyclopedia of Genes and Genomes (KEGG) pathway analysis was conducted (Figure 5B). Clearly, there were striking differences between the DAPs from the two different salt stress conditions. Under 200 mM NaCl treatment, most of DAPs involved in phenylpropanoid biosynthesis, glutathione metabolism, purine metabolism, and starch and sucrose metabolism pathways were differentially expressed. In contrast, under 400 mM NaCl treatment, most of DAPs involved in carbon fixation, glyoxylate and dicarboxylate metabolism, pyruvate metabolism, and methane metabolism pathways were differentially expressed. These results showed that different pathways were deployed under different salt stress conditions. Higher stress levels caused slowdown in biosynthesis and increase of cellular damage and catabolic activities. Under 200 mM NaCl treatment, five proteins (glutaredoxin-like isoform, ascorbate peroxidase, dehydroascorbate reductase, fasciclin-like arabinogalactan protein and glutathione s-transferase) associated with glutathione metabolism were identified. All the proteins except the glutaredoxin-like isoform, were increased, suggesting activation of glutathione metabolism under the 200mM NaCl. Among non-enzymatic antioxidants, glutathione is one of the most abundant soluble antioxidants in higher plants [36]. It plays a vital role as electron donors and scavenge ROS directly through ASA-GSH cycle [37]. However, under the 400 mM NaCl treatment, we didn't identify any DAPs associated with glutathione metabolism. This result supports that different pathways were deployed, and may indicate disfunction of antioxidant systems under high salt stress [36].

Subcellular localization analysis revealed that most of the DAPs were targeted to the chloroplast, nucleus and cell wall under the 200 mM NaCl treatment (Figure 5C). Under the 400 mM NaCl treatment, most of the DAPs were targeted to the chloroplast, plasma membrane and cytoplasm (Figure 5D). The different subcellular locations of the guard cell DAPs from the 200 mM and 400 mM NaCl treatments highlight differential regulations and plasticity of the guard cell proteome in response to different stress conditions. To further comprehend potential interactions among the DAPs, the STRING protein interaction database was used to analyze protein-protein interaction (PPI). Among the DAPs, six pathways were significantly enriched including: cysteine and methionine metabolism, RNA transport, carbon fixation, glyoxylate and dicarboxylate metabolism, spliceosome and ribosome (Figure 6). The interactions between proteins associated with spliceosome and ribosome appear to be more complicated, and most of these proteins were decreased.

Transcriptional analysis of the Genes Encoding the DAPs in Guard Cells

The utility of using enriched stomatal guard cells is to correlate guard cell molecular changes to the salt stress-induced stomatal movement. Here we focused on 16 DAPs potentially involved in stress response and stomatal movement. Five proteins were identified in both the 200 mM NaCl and 400 mM NaCl samples (i.e., glycine-rich cell wall structural protein-like, non-specific lipid-transfer protein , translation initiation factor IF-3 , ATP-dependent Clp protease proteolytic subunit and glycine-rich RNA-binding protein RZ1A), 5 were identified only in the 200 mM NaCl samples (i.e., DUF642, protein aspartic protease in guard cell 1, temperature-induced lipocalin, salt tolerance protein 5 and UPF0603 protein), and 6 were identified only in the 400 mM NaCl samples (i.e., salinity-induced protein, jasmonate-induced protein homolog, salt tolerance protein 6, cation/calcium exchanger 5, fasciclin-like arabinogalactan protein 10 and V-type proton ATPase subunit G).

To compare and contrast the changes at the transcription level and protein level of the 16 DAPs, we analyzed their transcription level changes using real-time PCR (Figure 7). Among the 10 DAPs under 200 mM NaCl treatment, the transcriptional levels of 7 genes were consistent with the corresponding protein level trend. The aspartic protease in guard cell 1, salt tolerance protein 5 and UPF0603 protein displayed different transcriptional changes from the corresponding protein level changes. Under the 400 mM NaCl treatment, among the 11 DAPs, 6 genes showed transcriptional changes inconsistent with the corresponding protein level changes. The inconsistency between the changes at the transcriptional level and at the protein level may be attributed to differential stability of the molecules, as well as posttranscriptional and/or posttranslational modifications.

Discussion

Soil salinity causes stomata closure, thereby leads to reducing CO_2 assimilation and yield penalty [29]. To date, a large number of studies have used proteomics to analyze intact tissues containing many different types of cells (such as leaves), thus masking guard cell-specific mechanisms underlying the stomatal movement under stress conditions. Currently, only a very limited number of studies have focused on proteomics and metabolomics changes in guard cells per se [25, 38-40], largely because of challenges associated with obtaining a sufficient number of isolated guard cells for the experiment. In this study, we developed a protocol suitable for *BvM14* line guard cell enrichment, and reported a comprehensive analysis of guard cell proteomic responses to salt stress through complex molecular mechanisms, including transcription, translation, and signal transduction of salt stress-related proteins (Figure 8).

Transcription and translation-related proteins

The transcriptional and translational control of gene expression in response to stress is an important process for plants to adapt to the environment. Three transcription factors (TFs) and eight RNA binding

proteins (RBPs) were identified in this study. Three TFs (A0A1S4B938, A0A2P6R6S9, D9ZJE7) were all decreased under salt stress, indicating salt stress affected gene transcription. Like TFs, RBPs also participate in various transcriptional RNA-binding events [41], especially Glycine-rich RNA-binding proteins (GR-RBP), which have been reported to play important roles in regulation of gene expression in plants under stresses [42-45]. Interestingly, GR-RBP has an effect on stomatal opening under salt stress, resulting in a negative effect on salt stress tolerance [42]. This data was consistent with our research results (A0A1U7ZD41). Therefore, we speculate that GR-RBP may interact with the mRNAs of genes, which are closely involved in stomatal closure in the guard cells, and modulate the processing and folding of the mRNAs in plants under different stress conditions.

We observed that translation initiation factor IF-3 (AOA1U8ADE4), translation initiation factor SUI1 (G7IY05) and translation elongation factor Ts (A0A200PQV0) were all decreased by salt stress. The changes in protein synthesis observed in this study support the notion that salt stress generally represses protein synthesis [46]. In addition, we also identified a number of ribosomal proteins that were decreased under salt stress. In Arabidopsis, plant growth were negatively correlated with ribosome abundance [47]. This is mainly because maintaining a high ribosomes content would cause a “waste” of energy [48]. Therefore, lower ribosome content allows energy use appropriately for salt stress responses.

Carbohydrate metabolism and energy-related proteins

Carbohydrate metabolism is closely related to plant stress response under adverse conditions. A large amount of energy needs to be provided for the stomatal movement of *BvM14* line under salt stress. Carbohydrate metabolism can provide ATP through glycolysis and tricarboxylic acid cycle (TCA cycle) [49]. Based on our results, four proteins, including Succinate-CoA ligase (AOAOK9RYN2), Succinate dehydrogenase (A0A1J6IM89), Malate dehydrogenase (A0A067GTM8) and Aspartate aminotransferase (A0A2K2A8I6), involved in TCA cycle were identified in the *BvM14* guard cells. Succinate-CoA ligase was increased under salt stress. It catalyzes the convertion of Sussinyl-CoA to Succinate and produces ATP at the same time [50]. Similarly, we also observed that Succinate dehydrogenase was increased under salt stress. It is one of the hinges connecting oxidative phosphorylation and electron transport, which can catalyze the reaction of succinate to fumarate and transfer electrons from succinate to ubiquinone (coenzyme Q) to finally produce ATP. This may promote the closure of stomata and help *BvM14* line to resist salt stress. However, malate dehydrogenase level was decreased under salt stress. This decrease may be due to the decrease in malate content during stomata closure [51-53]. At the same time, the decrease of oxaloacetate content may inhibit the TCA cycle. Therefore, the increased abundance of Aspartate aminotransferase that can catalyze the synthesis of oxaloacetate may make up for this gap to ensure the normal TCA cycle function. ATP synthase produces ATP from ADP when these is a proton gradient across the membrane. In our study three components of ATP synthase (A0A061DVA9, A0A061GHV4, H2BLF5) were increased under salt stress. V-type proton ATPase is an ion channel protein on the vacuole that relies on the energy produced by hydrolyzing ATP to transfer protons. In the present study, V-type proton ATPase (A0A2N9EW52) was present at high levels under salt stress providing a

proton motive force to impel excessive cytoplasmic Na^+ into vacuoles and has firm control over the ion compartmentalization by regulating the driving force of Na^+ transport.

It has been reported that guard cell photosynthesis is necessary for stomatal movement [54, 55]. Our proteomic analysis results identified five increased proteins involved in the light reactions of photosynthesis, including Photosystem Ⅱ Pbs27, photosystem Ⅰ PsaN and photosystem Ⅰ PsaN reaction center subunit N. The other two proteins were oxygen-evolving enhancer protein 2 and oxygen-evolving enhancer protein 3, which play important roles in response to salt stress and may contribute to ROS elimination. The light reaction of photosynthesis convers light into chemical energy, supplying ATP and NADPH to drive the carbon dioxide reduction and fixation processes [56]. The increase in ATP synthase epsilon chain under salt stress may indicate more energy is required for carbon assimilation [57]. Photosynthesis carbon assimilation is driven by ribulose bisphosphate carboxylase /oxygenase (RubisCO) activase [58]. Co-overexpressing gene *RCA* (RubisCO activase) and gene *AVP1* (Arabidopsis vacuolar pyrophosphatase) improved salinity-, drought-, and heat-tolerance in transgenic plants [59]. Our proteomic data identified three proteins involved in CO_2 assimilation, RubisCO activase, RubisCO large subunit and ribulose-phosphate 3-epimerase. All of them decreased under salt treatment, which is consistent with the previous results of decreased net photosynthetic rate under salt stress [60].

Stress-related proteins

Under salt stress, guard cells may sense signals from the roots. The combination of ABA and cysteine-rich receptor-like protein kinase (CRK) activates the expression of downstream SnRK2s and then activates S-type channel-associated 1 (SLAC1) activity to induce the stomatal closure (Figure 8). Here we found that Fasciclin-like arabinogalactan protein 10 (FLAs) was significantly increased under salt stress. It has been shown that under abiotic stress, FLAs and ABA can promote the increase of intracellular ROS and improve plant stress tolerance [61]. Meanwhile, ROS may increase cellular Ca^{2+} concentration. The Ca^{2+} spike in guard cells may act as second messenger together with EF-Hand to activate the SOS pathway in guard cells [62]. The Na^+/H^+ antiporter (SOS1) can transport the excess Na^+ out of the cell or compartmentalize it in the vacuole to prevent excessive salt buildup in the cystoplasm. Thus, the normal Na^+ level and pH in the cells can be maintained [63]. In addition, our results show that the expression of V-ATPase-1 was significantly increased under salt stress, which helps to sequester Na^+ into the vacuoles.

Although ROS usually play a signaling role in the process of plant response to abiotic stress, excessive ROS can cause irreversible damage to plant cell membranes and affect cellular functions. Based on our results, two important enzymes dehydroascorbate reductase (Q9FVE4) and ascorbate peroxidase (O81603) involved in the ascorbate-glutathione pathway were both increased under salt stress. As shown in Figure 8, their increased expression can effectively inhibit the accumulation of ROS and help guard cells to resist oxidative stress. In addition, we noticed a decrease in the expression of glutaredoxin (A0A1U8IAK4). Glutaredoxin (GRX) catalyzed deglutathionylation of protein-glutathione mixed disulfides (Protein-SSG) to produced GRX-SSG and release the non-glutathione part of protein (Protein-SH). GRX-

SSG is reduced by GSH and the product is GSSG [64, 65]. Obviously, GSH is required for both the deglutathionylation and ascorbate-glutathione pathways, so we speculate that the decreased expression of GRX is due to the priority of ROS clearance under salt stress.

Other changed proteins

In this study, the increase of S-adenosylmethionine synthase (Q4H1G4) under salt stress can promote the synthesis of S-adenosylmethionine. S-adenosylmethionine is an important methyl donor that can generate choline. Choline can be oxidized to generate betaine to enhance the plant's resistance to stress. The accumulation of betaine is indispensable for maintaining low intercellular osmotic potential and preventing the harmful effects of salt stress. In addition, we also identified two proteins involved in cell wall structure. One is DUF642 (A0A161DY72) is a highly conserved plant-specific family unknown cell wall-associated proteins. There is an evidence that DUF642 family regulates the activity of pectin methyl esterase [66]. Our data showed that decrease of DUF642, which may increase the thickness of cell wall of the guard cells and contribute to the stability of guard cell structure. The other is glycine-rich cell wall structural protein (GRP) (A0A1S4BC76), which the primary sequences contain more than 60% glycine. It has been reported that GRPs are structurally similar to collagen in animal and allow cell wall extensibility [67]. The decrease of GRP may promote stomatal closure.

Conclusion

In this study, we used the iTRAQ labeling quantitative proteomics to investigate the effects of salt stress on guard cell proteome of the *BvM14* line. We identified 80 and 72 DAPs involved in different biological processes, including gene expression, stress signaling, carbohydrate and energy metabolism under salt stress conditions. Higher level of salt stress caused different proteomic changes than lower concentration of salt. The study not only showed the utility of multiplexing of the iTRAQ LC-MS/MS technology in the study of guard cell protein changes in response to different salt treatments, but also revealed potential molecular mechanisms underlying the guard cell salt stress response in the *Bv*M14 plants (Fig. 8). Through real-time PCR validation of the DAPs, it became clear that the inconsistency between the changes at the transcriptional level and at the protein level may be attributed to differential stability of transcripts and proteins, as well as posttranscriptional and/or posttranslational modifications. Additionally, there were several differential proteins of unknown functions. Future research efforts should focus on validating the proposed molecular mechanisms, elucidating the functions of the unknown proteins, and improving crop salt stress tolerance through regulating guard cell functions.

Abbreviations

GCs
guard cells
ABA

abscisic acid
ROS
reactive oxygen species
BvM14 line
Sugar beet monosomic addition line M14
MeJA
methyljasmonate
DAPs
differentially abundant proteins
GO
Gene ontology
APX
Ascorbate Peroxidase
ASA
ascorbic acid
TFA
Trifluoroacetic acid
SPE
solid phase extraction
SCX
Strong Cation Exchange
LC-MS/MS
liquid chromatography tandem mass spectrometry
AHA1
H^+-ATPase
PSMs
peptide spectrum matches
nsLTP
Non-specific lipid-transfer protein
KEGG
Kyoto Encyclopedia of Genes and Genomes
PPI
protein-protein interaction

Declarations

CONFLICTS OF INTEREST

The authors declare no conflict of interest. The funders had no role in the design of the study; in the collection, analyses, or interpretation of data; in the writing of the manuscript; or in the decision to publish

the results.

Ethics approval and consent to participate

All methods were carried out in compliance with local and national regulations. Seeds of Sugar Beet Monosomic Addition Line M14 are stored in the Key Laboratory of Molecular Biology of Heilongjiang Province, College of Life Sciences, Heilongjiang University. The source of seeds and technology do not involve any ethical concerns.

Consent for publication

Not applicable

Availability of data and materials

The datasets generated and analysed during the current study are available in the ProteomeXchange repository, ProteomeXchange Datasets

Competing interests

The authors declare that they have no competing interests.

Funding

This research was supported by the National Science Foundation of China (Project 32072122 and project 31471552) to HL; by Project 31671751 to SC; by Project 31401441 to CM and by Project YJSCX2021-208HLJU to JZ

Authors' contributions

JZ wrote the first draft. XT conducted biochemical experiments and assisted with draft editing. JL, SW and HL assisted with draft editing. SC assisted with mass spectrometry and edited of the manuscript. Bing Yu analyzed data. HL and CM funded acquisition, projected supervision and finalized the manuscript. All authors read and approved the final manuscript.

Acknowledgements

We thank Hongli Li for useful suggestions, Huizi Duanmu reading the manuscript and providing helpful suggestions.

References

1. Geng, S., B.B. Misra, E. de Armas, D.V. Huhman, H.T. Alborn, L.W. Sumner, et al. Jasmonate-mediated stomatal closure under elevated CO_2 revealed by time-resolved metabolomics. Plant J. 2016;88(6):947-962. https://dx.doi.org/10.1111/tpj.13296.

2. Geng, S., B. Yu, N. Zhu, C. Dufresne, and S. Chen. Metabolomics and Proteomics of *Brassica napus* Guard Cells in Response to Low CO_2. Front Mol Biosci. 2017;4:51. https://dx.doi.org/10.3389/fmolb.2017.00051.
3. Wu, G., J. Wang, R. Feng, S. Li, and C. Wang. iTRAQ-Based comparative proteomic analysis provides insights into molecular mechanisms of salt tolerance in Sugar Beet (*Beta vulgaris* L.). Int J Mol Sci. 2018;19(12):3866. https://dx.doi.org/10.3390/ijms19123866.
4. Munns, R. and M. Tester. Mechanisms of salinity tolerance. Annu Rev Plant Biol. 2008;59:651-681. https://dx.doi.org/10.1146/annurev.arplant.59.032607.092911.
5. Kim, T.H., M. Böhmer, H.H. Hu, N. Nishimura, and J.I. Schroeder. Guard cell signal transduction network: advances in understanding abscisic acid, CO_2, and Ca^{2+} signaling. Annu Rev Plant Biol. 2010;61:561-591. https://dx.doi.org/10.1146/annurev-arplant-042809-112226.
6. Sah, S.K., K.R. Reddy, and J.X. Li. Abscisic acid and abiotic stress tolerance in crop plants. Front Plant Sci. 2016;7:571. https://dx.doi.org/10.3389/fpls.2016.00571.
7. Albacete, A., M.E. Ghanem, C. Martínez-Andújar, M. Acosta, J. Sánchez-Bravo, V. Martínez, et al. Hormonal changes in relation to biomass partitioning and shoot growth impairment in salinized tomato (*Solanum lycopersicum* L.) plants. J Exp Bot. 2008;59(15):4119-4131. https://dx.doi.org/10.1093/jxb/ern251.
8. Skorupa, M., M. Gołębiewski, K. Kurnik, J. Niedojadło, J. Kęsy, K. Klamkowski, et al. Salt stress vs. salt shock - the case of sugar beet and its halophytic ancestor. BMC Plant Biol. 2019;19(1):57. https://dx.doi.org/10.1186/s12870-019-1661-x.
9. Li, H., H. Cao, Y. Wang, Q. Pang, C. Ma, and S. Chen. Proteomic analysis of sugar beet apomictic monosomic addition line M14. J Proteomics. 2009;73(2):297-308. https://dx.doi.org/10.1016/j.jprot.2009.09.012.
10. Yang, L., C. Ma, L. Wang, S. Chen, and H. Li. Salt stress induced proteome and transcriptome changes in sugar beet monosomic addition line M14. J Plant Physiol. 2012;169(9):839-50. https://dx.doi.org/10.1016/j.jplph.2012.01.023.
11. Yu, B., J. Li, J. Koh, C. Dufresne, N. Yang, S. Qi, et al. Quantitative proteomics and phosphoproteomics of sugar beet monosomic addition line M14 in response to salt stress. J Proteomics. 2016;143:286-297. https://dx.doi.org/10.1016/j.jprot.2016.04.011.
12. Yang, L., Y. Zhang, N. Zhu, J. Koh, C. Ma, Y. Pan, et al. Proteomic analysis of salt tolerance in sugar beet monosomic addition line M14. J Proteome Res. 2013;12(11):4931-4950. https://dx.doi.org/10.1021/pr400177m.
13. Li, H., Y. Pan, Y. Zhang, C. Wu, C. Ma, B. Yu, et al. Salt stress response of membrane proteome of sugar beet monosomic addition line M14. J Proteomics. 2015;127:18-33. https://dx.doi.org/10.1016/j.jprot.2015.03.025.
14. Zhu, M., N. Zhu, W.Y. Song, A.C. Harmon, S.M. Assmann, and S. Chen. Thiol-based Redox Proteins in *Brassica napus* Guard Cell Abscisic Acid and Methyl Jasmonate Signaling. Plant J. 2014;78(3):491-515. https://dx.doi.org/10.1111/tpj.12490.

15. Zhang, T., M. Zhu, N. Zhu, J.M. Strul, C.P. Dufresne, J.D. Schneider, et al. Identification of thioredoxin targets in guard cell enriched epidermal peels using cysTMT proteomics. J Proteomics. 2016;133:48-53. https://dx.doi.org/10.1016/j.jprot.2015.12.008.
16. Ghoulam, C., A. Foursy, and K. Fares. Effects of salt stress on growth, inorganic ions and proline accumulation in relation to osmotic adjustment in five sugar beet cultivars. Environ Exp Bot. 2002;47:39-50.
17. Rocco, M., C. D'Ambrosio, S. Arena, M. Faurobert, A. Scaloni, and M. Marra. Proteomic analysis of tomato fruits from two ecotypes during ripening. Proteomics. 2006;6(13):3781-3791. https://dx.doi.org/10.1002/pmic.200600128.
18. Jiao, C. and Z. Gu. iTRAQ-based proteomic analysis reveals changes in response to sodium nitroprusside treatment in soybean sprouts. Food Chem. 2019;292:372-376. https://dx.doi.org/10.1016/j.foodchem.2018.02.054.
19. Pang, Q.Y., S.X. Chen, S.J. Dai, Y.Z. Chen, Y. Wang, and X.F. Yan. Comparative proteomics of salt tolerance in *Arabidopsis thaliana* and *Thellungiella halophila.* J Proteome Res. 2010;9(5):2584-2599. https://dx.doi.org/10.1021/pr100034f.
20. Parker, J., N. Zhu, M. Zhu, and S. Chen. Profiling thiol redox proteome using isotope tagging mass spectrometry. J Vis Exp. 2012;61(61):e3766. https://dx.doi.org/10.3791/3766.
21. Perez-Riverol, Y., A. Csordas, J. Bai, M. Bernal-Llinares, S. Hewapathirana, D.J. Kundu, et al. The PRIDE database and related tools and resources in 2019: improving support for quantification data. Nucleic Acids Res. 2019;47(1):D442-d450. https://dx.doi.org/10.1093/nar/gky1106.
22. Untergasser, A., H. Nijveen, X. Rao, T. Bisseling, R. Geurts, and J.A. Leunissen. Primer3Plus, an enhanced web interface to Primer3. Nucleic Acids Res. 2007;35W71-W74. https://dx.doi.org/10.1093/nar/gkm306.
23. Pichon, M., A. Gaymard, L. Josset, M. Valette, G. Millat, B. Lina, et al. Characterization of oseltamivir-resistant influenza virus populations in immunosuppressed patients using digital-droplet PCR: Comparison with qPCR and next generation sequencing analysis. Antiviral Res. 2017;145:160-167. https://dx.doi.org/10.1016/j.antiviral.2017.07.021.
24. Lawrence, S., Q. Pang, W. Kong, and S. Chen. Stomata Tape-Peel: An Improved Method for Guard Cell Sample Preparation. J Vis Exp. 2018;(137):https://dx.doi.org/10.3791/57422.
25. Zhu, M., S. Dai, S. McClung, X. Yan, and S. Chen. Functional differentiation of *Brassica napus* guard cells and mesophyll cells revealed by comparative proteomics. Mol Cell Proteomics. 2009;8(4):752-766. https://dx.doi.org/10.1074/mcp.M800343-MCP200.
26. Rasouli, F., A. Kiani-Pouya, H. Zhang, and S. Shabala. Developing and validating protocols for mechanical isolation of guard-cell enriched epidermal peels for omics studies. Funct Plant Biol. 2020;47(9):803-814. https://dx.doi.org/10.1071/fp20085.
27. Wiśniewska, E. and A. Majewska-Sawka. Arabinogalactan-proteins stimulate the organogenesis of guard cell protoplasts-derived callus in sugar beet. Plant Cell Rep. 2007;26(9):1457-1467. https://dx.doi.org/10.1007/s00299-007-0348-1.

28. Franzisky, B.L., C.M. Geilfus, M.L. Romo-Pérez, I. Fehrle, A. Erban, J. Kopka, et al. Acclimatisation of guard cell metabolism to long-term salinity. Plant Cell Environ. 2021;44(3):870-884. https://dx.doi.org/10.1111/pce.13964.
29. Hedrich, R. and S. Shabala. Stomata in a saline world. Curr Opin Plant Biol. 2018;46:87-95. https://dx.doi.org/10.1016/j.pbi.2018.07.015.
30. Xu, M. The optimal atmospheric CO_2 concentration for the growth of winter wheat (*Triticum aestivum*). J Plant Physiol. 2015;184:89-97. https://dx.doi.org/10.1016/j.jplph.2015.07.003.
31. Keane, P.J., N. Limonglello, and M.A. Warren. A modified method for clearing and staining leaf-infecting fungi in whole leaves. Australasian Plant Pathology. 1988;17(2):37-38.
32. Sarowar, S., Y.J. Kim, K.D. Kim, B.K. Hwang, S.H. Ok, and J.S. Shin. Overexpression of lipid transfer protein (LTP) genes enhances resistance to plant pathogens and LTP functions in long-distance systemic signaling in tobacco. Plant Cell Rep. 2009;28(3):419-427. https://dx.doi.org/10.1007/s00299-008-0653-3.
33. Choi, Y.E., S. Lim, H.J. Kim, J.Y. Han, M.H. Lee, Y. Yang, et al. Tobacco *NtLTP1*, a glandular-specific lipid transfer protein, is required for lipid secretion from glandular trichomes. Plant J. 2012;70(3):480-491. https://dx.doi.org/10.1111/j.1365-313X.2011.04886.x.
34. Guo, L., H. Yang, X. Zhang, and S. Yang. *Lipid transfer protein 3* as a target of MYB96 mediates freezing and drought stress in *Arabidopsis.* J Exp Bot. 2013;64(6):1755-1767. https://dx.doi.org/10.1093/jxb/ert040.
35. Jia, W., Q. Shi, R. Zhang, L. Shi, and X. Chu. Unraveling proteome changes of irradiated goat meat and its relationship to off-flavor analyzed by high-throughput proteomics analysis. Food Chem. 2021;337:127806. https://dx.doi.org/10.1016/j.foodchem.2020.127806.
36. Hasanuzzaman, M., M. Bhuyan, F. Zulfiqar, A. Raza, S.M. Mohsin, J.A. Mahmud, et al. Reactive Oxygen Species and Antioxidant Defense in Plants under Abiotic Stress: Revisiting the Crucial Role of a Universal Defense Regulator. Antioxidants (Basel). 2020;9(8):https://dx.doi.org/10.3390/antiox9080681.
37. Hasanuzzaman, M., M. Bhuyan, T.I. Anee, K. Parvin, K. Nahar, J.A. Mahmud, et al. Regulation of Ascorbate-Glutathione Pathway in Mitigating Oxidative Damage in Plants under Abiotic Stress. Antioxidants (Basel). 2019;8(9):https://dx.doi.org/10.3390/antiox8090384.
38. Zhao, Z., W. Zhang, B.A. Stanley, and S.M. Assmann. Functional proteomics of *Arabidopsis thaliana* guard cells uncovers new stomatal signaling pathways. Plant Cell. 2008;20(12):3210-3226. https://dx.doi.org/10.1105/tpc.108.063263.
39. Zhao, Z., B.A. Stanley, W. Zhang, and S.M. Assmann. ABA-regulated G protein signaling in *Arabidopsis* guard cells: a proteomic perspective. J Proteome Res. 2010;9(4):1637-1647. https://dx.doi.org/10.1021/pr901011h.
40. Geilfus, C.M., J. Lan, and S. Carpentier. Dawn regulates guard cell proteins in *Arabidopsis thaliana* that function in ATP production from fatty acid beta-oxidation. Plant Mol Biol. 2018;98(6):525-543. https://dx.doi.org/10.1007/s11103-018-0794-x.

41. Xiao, R., J.Y. Chen, Z. Liang, D. Luo, G. Chen, Z.J. Lu, et al. Pervasive Chromatin-RNA Binding Protein Interactions Enable RNA-Based Regulation of Transcription. Cell. 2019;178(1):107-121.e18. https://dx.doi.org/10.1016/j.cell.2019.06.001.
42. Kim, J.S., H.J. Jung, H.J. Lee, K.A. Kim, C.H. Goh, Y. Woo, et al. Glycine-rich RNA-binding protein 7 affects abiotic stress responses by regulating stomata opening and closing in *Arabidopsis thaliana.* Plant J. 2008;55(3):455-466. https://dx.doi.org/10.1111/j.1365-313X.2008.03518.x.
43. Kim, M.K., H.J. Jung, D.H. Kim, and H. Kang. Characterization of glycine-rich RNA-binding proteins in *Brassica napus* under stress conditions. Physiol Plant. 2012;146(3):297-307. https://dx.doi.org/10.1111/j.1399-3054.2012.01628.x.
44. Wang, B., G. Wang, F. Shen, and S. Zhu. A Glycine-Rich RNA-Binding Protein, CsGR-RBP3, Is Involved in Defense Responses Against Cold Stress in Harvested Cucumber (*Cucumis sativus* L.) Fruit. Front Plant Sci. 2018;9:540. https://dx.doi.org/10.3389/fpls.2018.00540.
45. Streitner, C., L. Hennig, C. Korneli, and D. Staiger. Global transcript profiling of transgenic plants constitutively overexpressing the RNA-binding protein *At*GRP7. BMC Plant Biol. 2010;10:221. https://dx.doi.org/10.1186/1471-2229-10-221.
46. Tuteja, N. Mechanisms of high salinity tolerance in plants. Methods Enzymol. 2007;428:419-438. https://dx.doi.org/10.1016/s0076-6879(07)28024-3.
47. Ishihara, H., T.A. Moraes, E.T. Pyl, W.X. Schulze, T. Obata, A. Scheffel, et al. Growth rate correlates negatively with protein turnover in Arabidopsis accessions. Plant J. 2017;91(3):416-429. https://dx.doi.org/10.1111/tpj.13576.
48. Schulze, W.X., M. Altenbuchinger, M. He, M. Kränzlein, and C. Zörb. Proteome profiling of repeated drought stress reveals genotype-specific responses and memory effects in maize. Plant Physiol Biochem. 2021;159:67-79. https://dx.doi.org/10.1016/j.plaphy.2020.12.009.
49. Höper, D., J. Bernhardt, and M. Hecker. Salt stress adaptation of Bacillus subtilis: a physiological proteomics approach. Proteomics. 2006;6(5):1550-62. https://dx.doi.org/10.1002/pmic.200500197.
50. Johnson, J.D., J.G. Mehus, K. Tews, B.I. Milavetz, and D.O. Lambeth. Genetic evidence for the expression of ATP- and GTP-specific succinyl-CoA synthetases in multicellular eucaryotes. J Biol Chem. 1998;273(42):27580-6. https://dx.doi.org/10.1074/jbc.273.42.27580.
51. Lee, M., Y. Choi, B. Burla, Y.Y. Kim, B. Jeon, M. Maeshima, et al. The ABC transporter AtABCB14 is a malate importer and modulates stomatal response to CO_2. Nat Cell Biol. 2008;10(10):1217-1223. https://dx.doi.org/10.1038/ncb1782.
52. Penfield, S., S. Clements, K.J. Bailey, A.D. Gilday, R.C. Leegood, J.E. Gray, et al. Expression and manipulation of *PHOSPHOENOLPYRUVATE CARBOXYKINASE 1* identifies a role for malate metabolism in stomatal closure. Plant J. 2012;69(4):679-688. https://dx.doi.org/10.1111/j.1365-313X.2011.04822.x.
53. Daloso, D.M., D.B. Medeiros, L. Dos Anjos, T. Yoshida, W.L. Araújo, and A.R. Fernie. Metabolism within the specialized guard cells of plants. New Phytol. 2017;216(4):1018-1033. https://dx.doi.org/10.1111/nph.14823.

54. Santelia, D. and T. Lawson. Rethinking Guard Cell Metabolism. Plant Physiol. 2016;172(3):1371-1392. https://dx.doi.org/10.1104/pp.16.00767.

55. Iwai, S., S. Ogata, N. Yamada, M. Onjo, K. Sonoike, and K.I. Shimazaki. Guard cell photosynthesis is crucial in abscisic acid-induced stomatal closure. Plant Direct. 2019;3(5):e00137. https://dx.doi.org/10.1002/pld3.137.

56. Matuszyńska, A., N.P. Saadat, and O. Ebenhöh. Balancing energy supply during photosynthesis - a theoretical perspective. Physiol Plant. 2019;166(1):392-402. https://dx.doi.org/10.1111/ppl.12962.

57. Liu, Y., Z. Shen, M. Simon, H. Li, D. Ma, X. Zhu, et al. Comparative Proteomic Analysis Reveals the Regulatory Effects of H_2S on Salt Tolerance of Mangrove Plant *Kandelia obovata.* Int J Mol Sci. 2019;21(1):118. https://dx.doi.org/10.3390/ijms21010118.

58. Andersson, I. and A. Backlund. Structure and function of Rubisco. Plant Physiol Biochem. 2008;46(3):275-291. https://dx.doi.org/10.1016/j.plaphy.2008.01.001.

59. Wijewardene, I., N. Mishra, L. Sun, J. Smith, X. Zhu, P. Payton, et al. Improving drought-, salinity-, and heat-tolerance in transgenic plants by co-overexpressing Arabidopsis vacuolar pyrophosphatase gene *AVP1* and Larrea Rubisco activase gene *RCA.* Plant Sci. 2020;296:110499. https://dx.doi.org/10.1016/j.plantsci.2020.110499.

60. Shen, Z., J. Chen, K. Ghoto, W. Hu, G. Gao, M. Luo, et al. Proteomic analysis on mangrove plant *Avicennia marina* leaves reveals nitric oxide enhances the salt tolerance by up-regulating photosynthetic and energy metabolic protein expression. Tree Physiol. 2018;38(11):1605-1622. https://dx.doi.org/10.1093/treephys/tpy058.

61. Xue, H. and G.J. Seifert. FASCICLIN LIKE ARABINOGALACTAN PROTEIN 4 and RESPIRATORY BURST OXIDASE HOMOLOG D and F independently modulate abscisic acid signaling. Plant Signal Behav. 2015;10(2):e989064. https://dx.doi.org/10.4161/15592324.2014.989064.

62. Cao, Y., M. Zhang, X. Liang, F. Li, Y. Shi, X. Yang, et al. Natural variation of an EF-hand Ca^{2+}-binding-protein coding gene confers saline-alkaline tolerance in maize. Nat Commun. 2020;11(1):186. https://dx.doi.org/10.1038/s41467-019-14027-y.

63. Apse, M.P., G.S. Aharon, W.A. Snedden, and E. Blumwald. Salt tolerance conferred by overexpression of a vacuolar Na^+/H^+ antiport in *Arabidopsis.* Science. 1999;285(5431):1256-1258. https://dx.doi.org/10.1126/science.285.5431.1256.

64. Gallogly, M.M., D.W. Starke, A.K. Leonberg, S.M. Ospina, and J.J. Mieyal. Kinetic and mechanistic characterization and versatile catalytic properties of mammalian glutaredoxin 2: implications for intracellular roles. Biochemistry. 2008;47(42):11144-57. https://dx.doi.org/10.1021/bi800966v.

65. Johansson, C., C.H. Lillig, and A. Holmgren. Human mitochondrial glutaredoxin reduces S-glutathionylated proteins with high affinity accepting electrons from either glutathione or thioredoxin reductase. J Biol Chem. 2004;279(9):7537-43. https://dx.doi.org/10.1074/jbc.M312719200.

66. Zúñiga-Sánchez, E., D. Soriano, E. Martínez-Barajas, A. Orozco-Segovia, and A. Gamboa-deBuen. *BIIDXI*, the *At4g32460* DUF642 gene, is involved in pectin methyl esterase regulation during

Arabidopsis thaliana seed germination and plant development. BMC Plant Biol. 2014;14:338. https://dx.doi.org/10.1186/s12870-014-0338-8.

67. Ringli, C., B. Keller, and U. Ryser. Glycine-rich proteins as structural components of plant cell walls. Cell Mol Life Sci. 2001;58(10):1430-1441. https://dx.doi.org/10.1007/pl00000786.

Figures

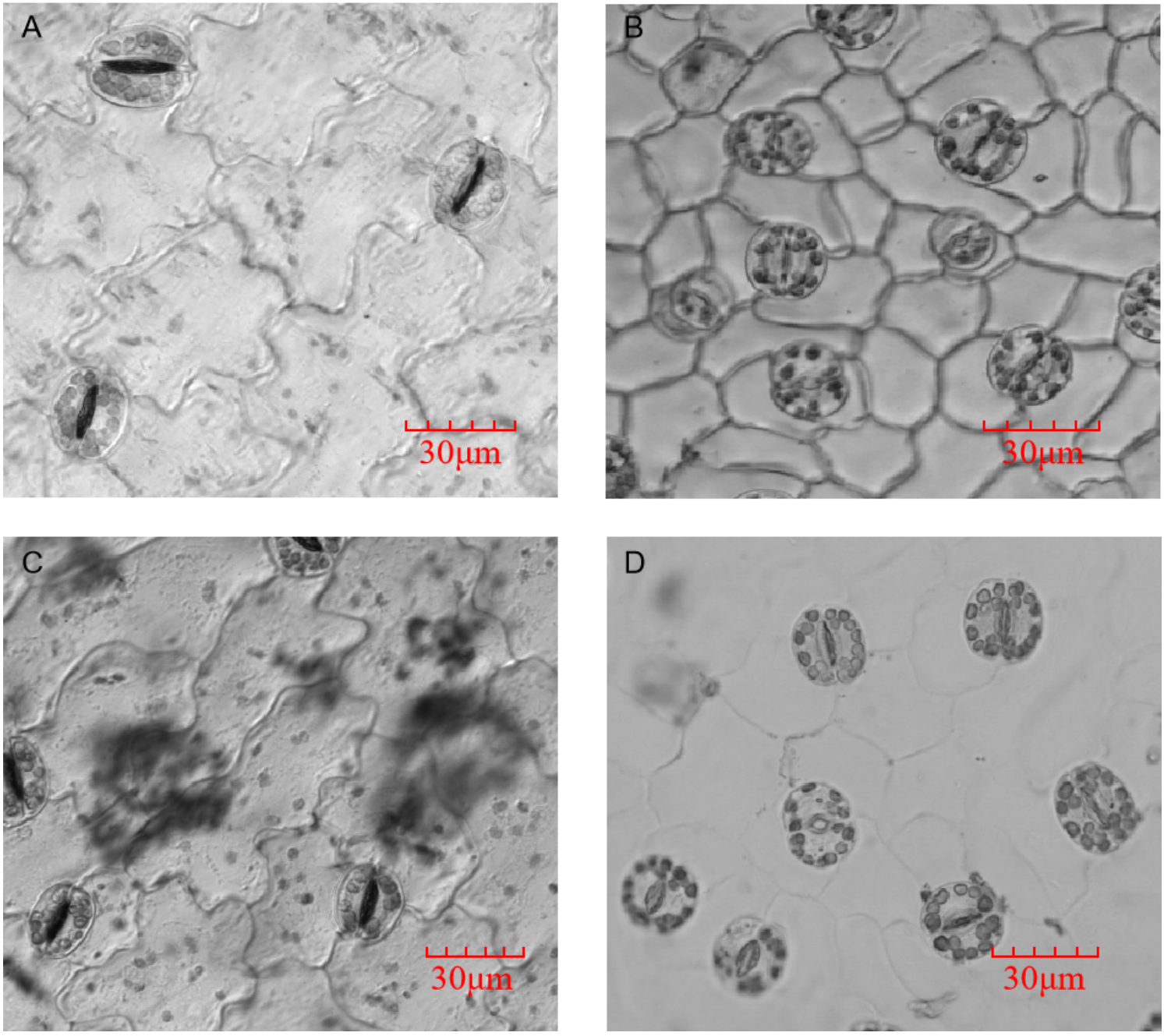

Figure 1

Comparison of the enrichment of sugar beet M14 guard cells from two different methods. Epidermal fragments obtained through the transparent tape-peeling method (A) and the blender pulverization

method (B). Images of the epidermal fragments after enzymolysis obtained through the transparent tape tearing method (C) and the blender pulverization method (D).

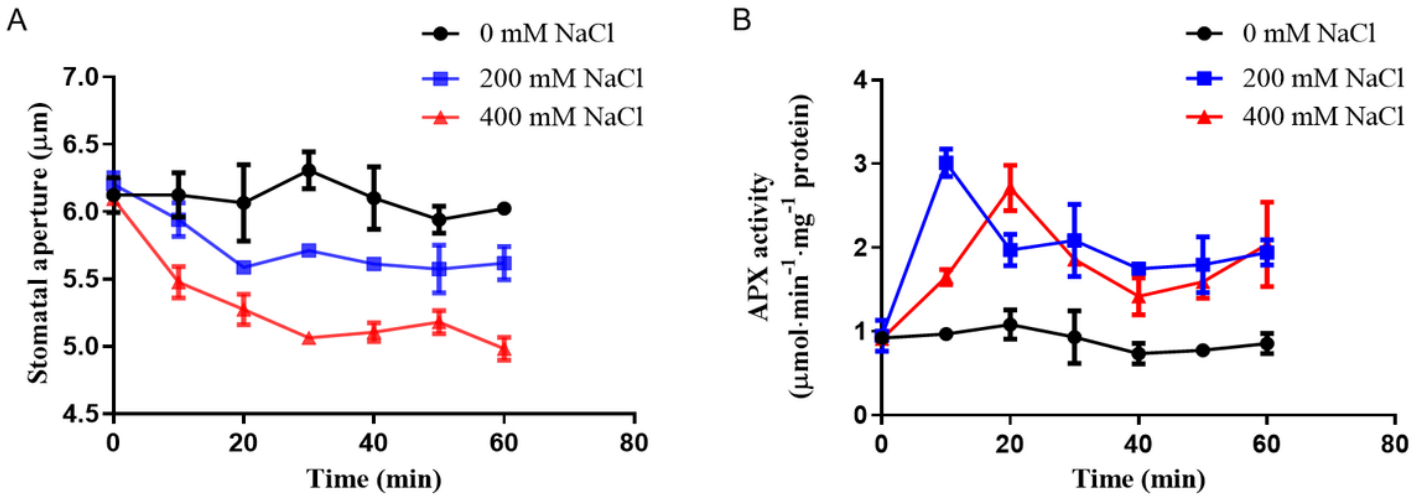

Figure 2

Stomatal aperture and APX enzyme activity at different time-points after different NaCl treatments. (A) Stomatal aperture at each time-point under 200 mM and 400 mM NaCl treatment. (B) APX enzyme activity at each time-point under 200 mM and 400 mM NaCl treatment. The error bars indicate standard error from three replicates.

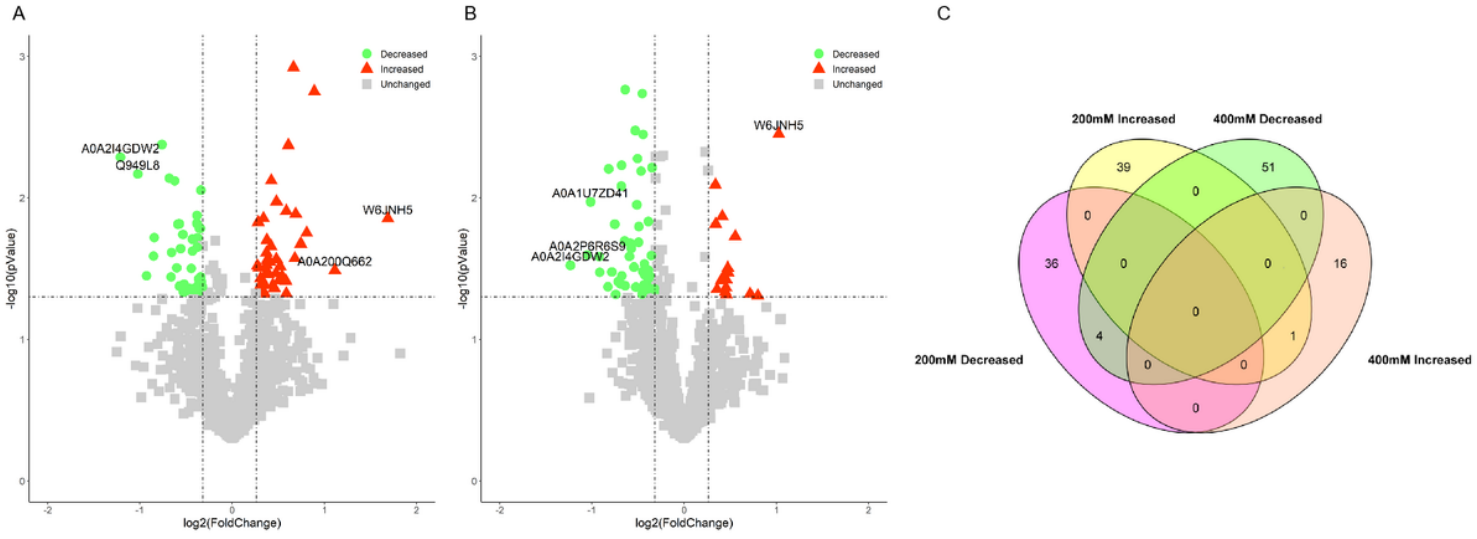

Figure 3

Abundance analysis of the differential abundant proteins (DAPs) under salt stress treatments. Abundance patterns of DAPs under 200 mM NaCl (A) and 400 mM NaCl (B) treatment. Each point represents the difference in relative protein levels between the two groups. Proteins labeled green (decreased) and red (increased) show significant differences between control and treatment groups. Veen diagrams showing the overlap of DAPs between 200 mM and 400 mM NaCl treatment samples (C).

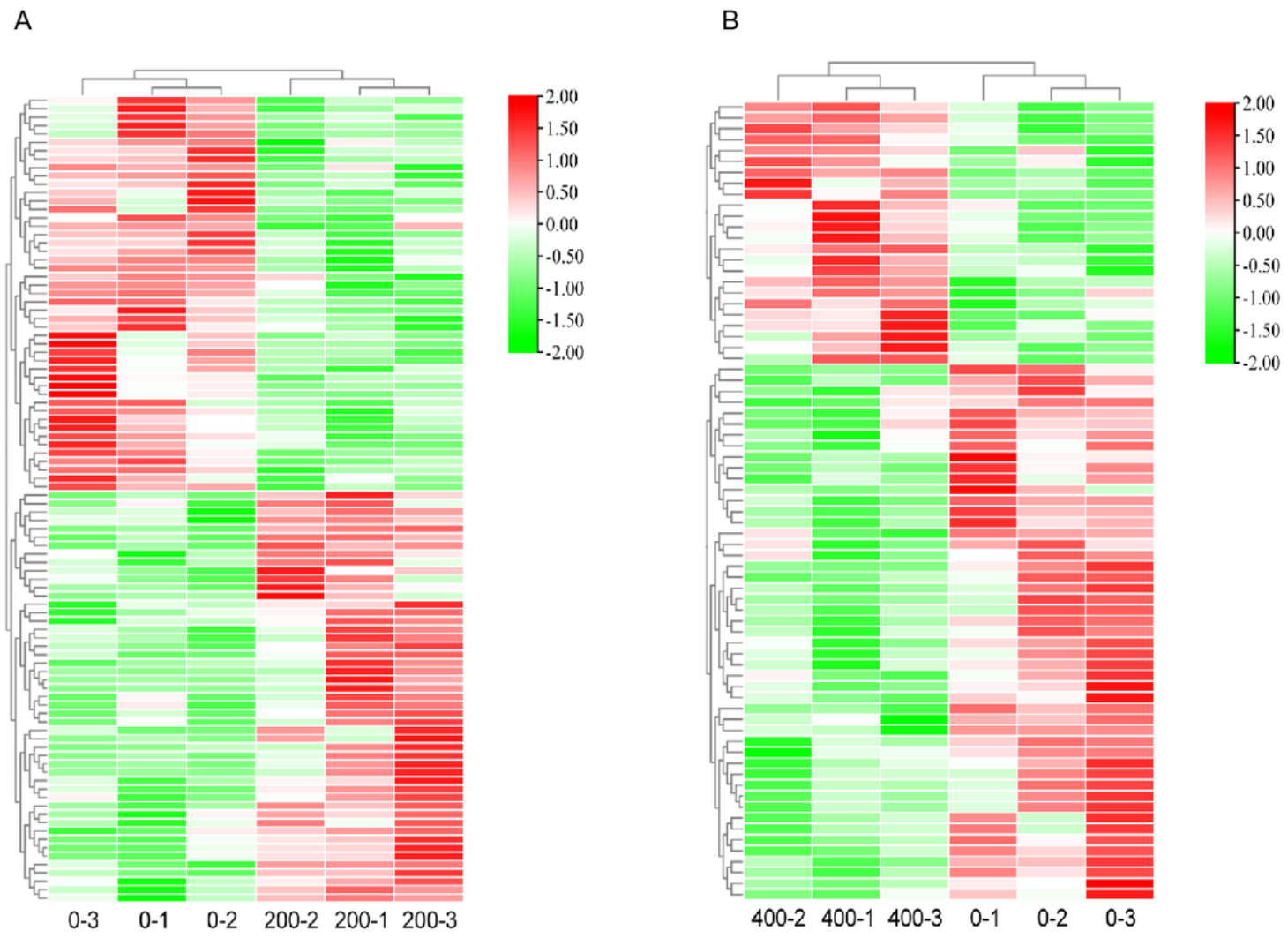

Figure 4

Hierarchial clustering of the DAPs in guard cells. DAPs under the 200 mM NaCl treatment compared with controls (A) and under the 400 mM NaCl treatment compared with controls (B). Different colors represent different relative protein abundances, with red and green indicating high and low abundances, respectively.

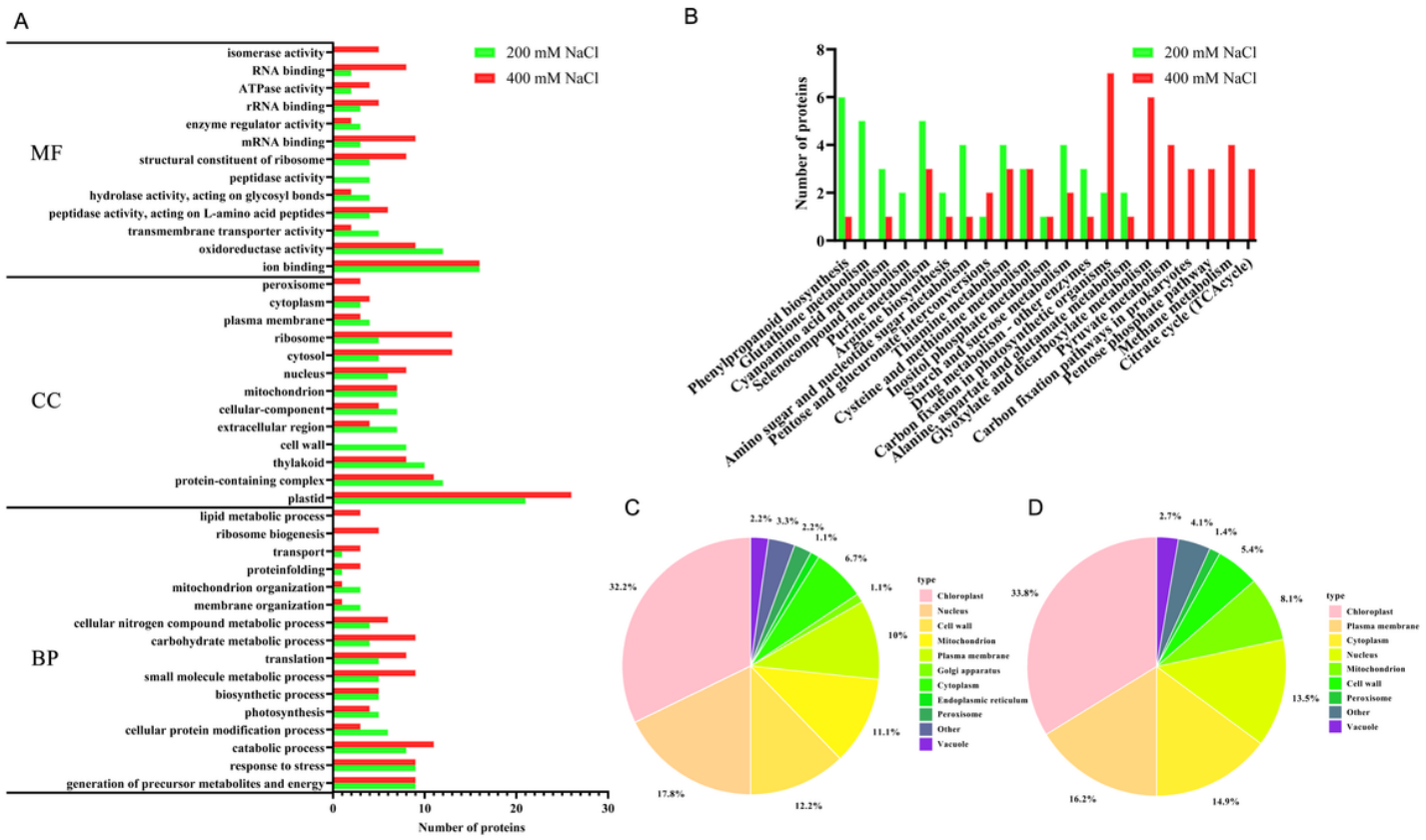

Figure 5

Bioinformatic analyses of the DAPs in guard cells. Gene Ontology (GO) classification of DAPs under the 200 mM NaCl treatment compared with 400 mM NaCl treatment (A), MF: Molecular function; CC: Cellular component; BP: Biological process. Kyoto Encyclopedia of Genes and Genomes (KEGG) pathway analysis of the DAPs under the 200 mM NaCl treatment compared with 400 mM NaCl treatment (B). Subcellular localization map of the DAPs under the 200 mM NaCl treatment (C) and 400 mM NaCl treatment (D).

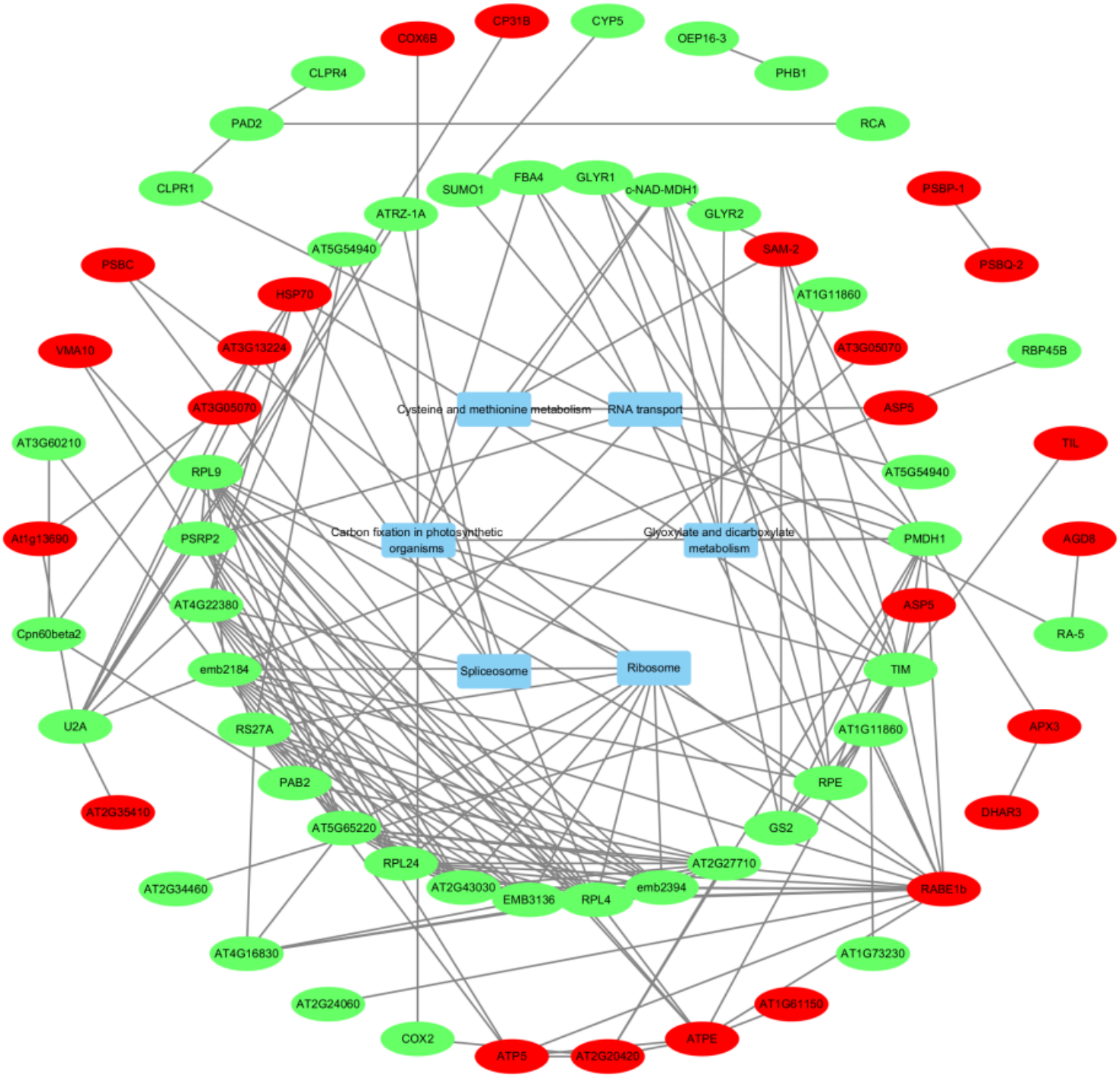

Figure 6

Protein-protein interaction (PPI) analysis of the DAPs under the salt stress treatments. PPI analysis of the DAPs using the *Arabidopsis thaliana* Plant Interaction Database. Rounded rectangles represent KEGG pathway. Oval represents proteins (red=increased protein; green=decreased protein). Lines show interactions between multiple proteins or between proteins and pathways. Please refer to Supplemental Table S2 for abbreviations.

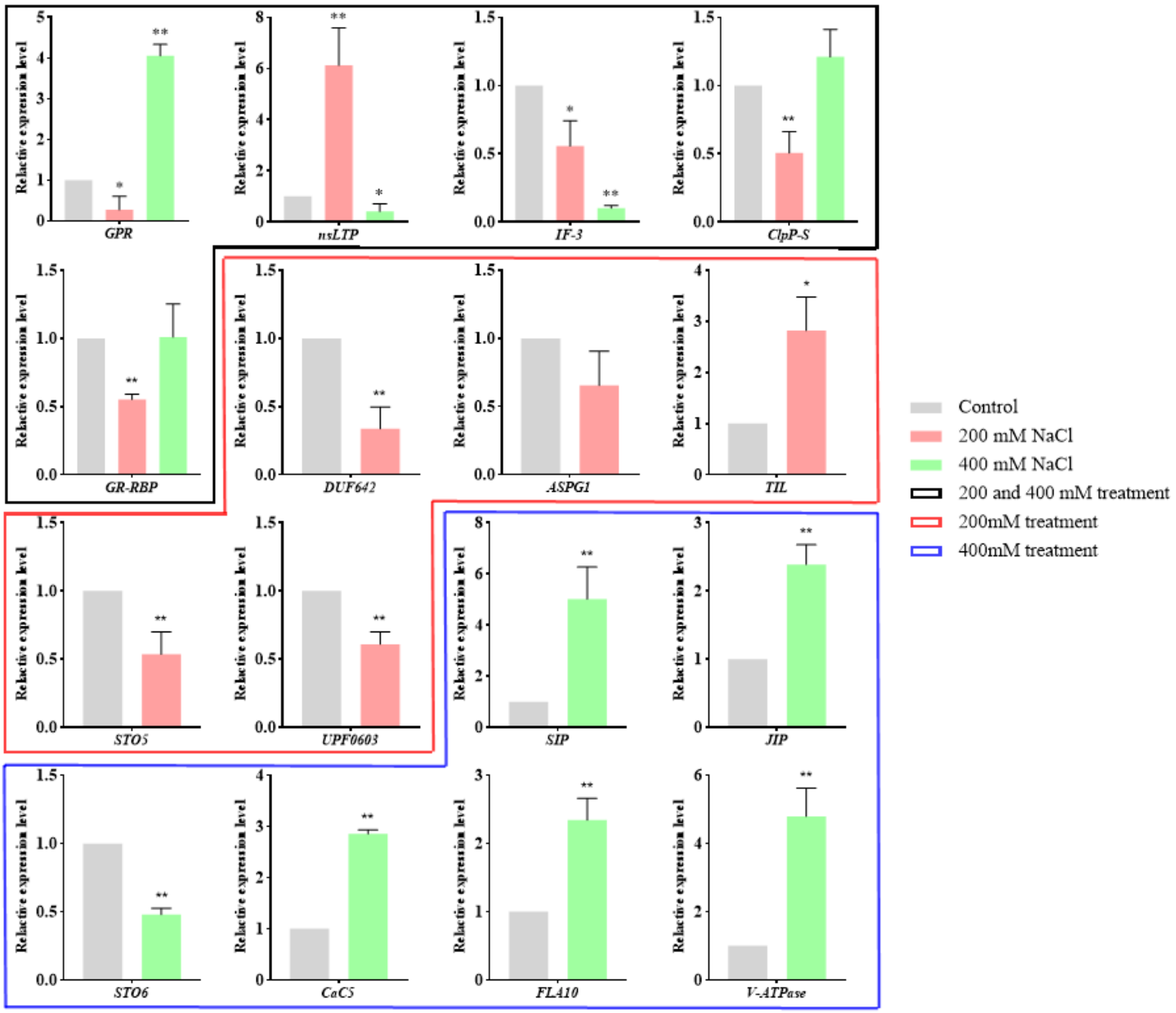

Figure 7

Relative quantification of the transcriptional levels of 16 DAP-encoding genes in guard cells after NaCl treatment. Statistical analyses were performed based on ANOVA; *P<0.05, **P<0.01. *GPR*, glycine-rich cell wall structural protein-like; *nsLTP*, non-specific lipid-transfer protein; *IF-3*, translation initiation factor; *ClpP-S*, ATP-dependent Clp protease proteolytic subunit; *GR-RBP*, glycine-rich RNA-binding protein RZ1A; *DUF642*, domain of unknow function 642; *ASPG1*, aspartic protease in guard cell 1; *TIL*, temperature-induced lipocalin; *STO*, salt tolerance protein ; *SIP*, salinity-induced protein; *JIP*, jasmonate-induced protein homolog; *CaC5*, cation/calcium exchanger 5; *FLA10*, fasciclin-like arabinogalactan protein 10; *V-ATPase*, V-type proton ATPase subunit G.

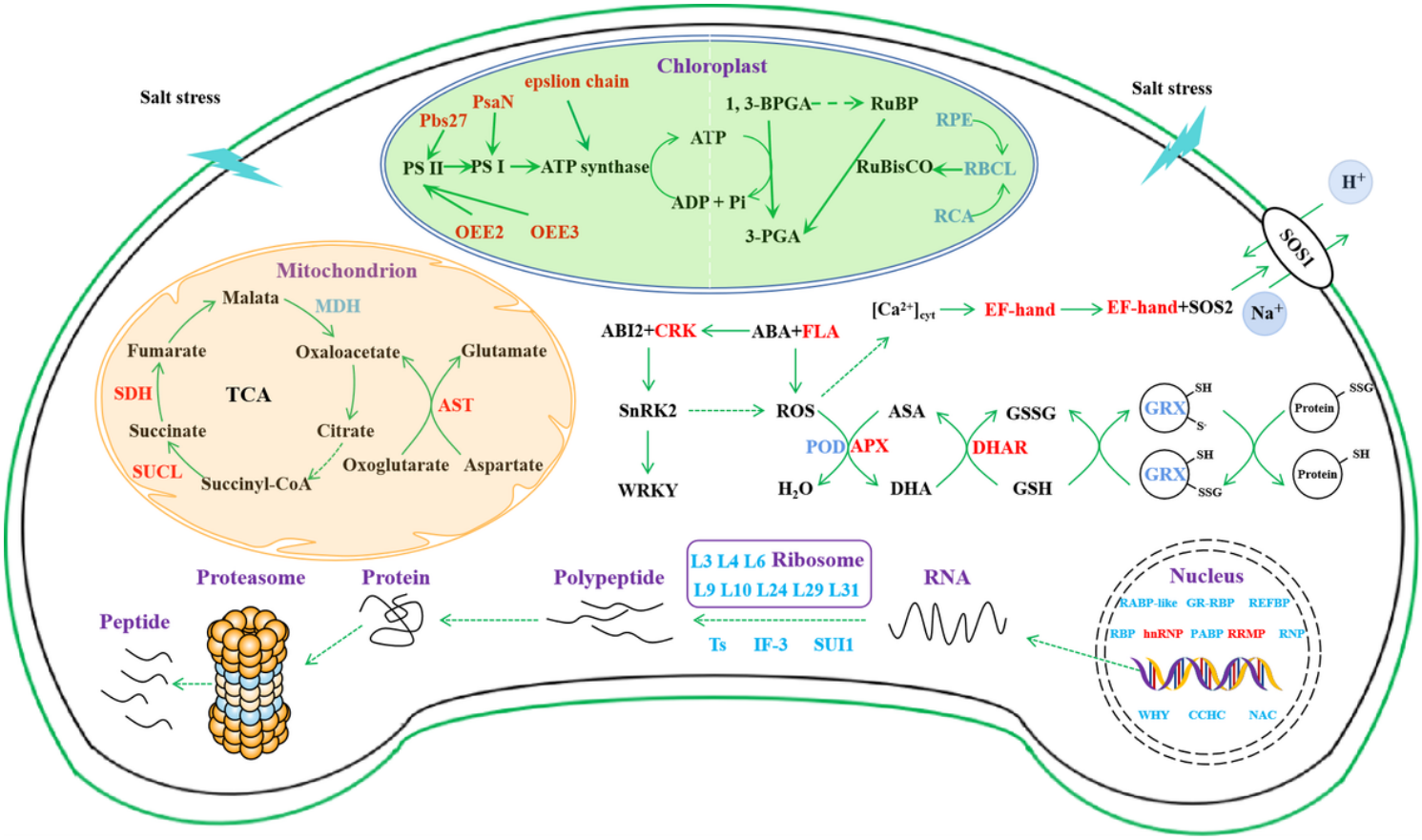

Figure 8

Proposed signaling pathway map of the DAPs in guard cells of sugar beet M14 under salt stress. The red and blue highlighted proteins indicate increased and decreased proteins, respectively. The dashed lines represent multiple steps. Abbreviations: Pbs27, Photosystem Ⅱ Pbs27; PsaN, photosystem Ⅰ PsaN; epsilon chain, ATP synthase epsilon chain; PS Ⅱ, Photosystem Ⅱ; PS Ⅰ, Photosystem Ⅰ; 1,3-BPGA, 1,3-bisphosphoglycerate; 3-PGA, 3-phosphoglycerate; RuBP, ribulose-1,5-bisphosphate; RuBisCO, ribulose-1,5-bisphosphate carboxylase/oxygenase; RPE, ribulose-phosphate 3-epimerase; RBCL, RubisCO large subunit; RCA, RubisCO activase; OEE2, oxygen-evolving enhancer protein 2; OEE3, oxygen-evolving enhancer protein 3; MDH, malate dehydrogenase; TCA, tricarboxylic acid; SDH, succinate dehydrogenase; SUCL, succinate-CoA ligase; AST, aspartate aminotransferase; ABI2, ABA-insensitive 2; CRK, cysteine-rich receptor-like protein kinase; SnRK2, SNF1-related protein kinase 2; ABA, abscisic acid; FLA, fasciclin-like arabinogalactan protein 10; ROS, reactive oxygen species; POD, peroxidase; APX, ascorbate peroxidase; ASA, ascorbate; DHA, dehydroascorbate; DHAR, dehydroascorbate reductase; GSH, glutathione; GSSG, glutathione disulfide; GRX, glutaredoxin; $[Ca^{2+}]$cyt, cytosolic calcium concentration; SOS2, salt-overly-sensitive 2; SOS1, salt-overly-sensitive 1.

Supplementary Files

This is a list of supplementary files associated with this preprint. Click to download.

- FigureS1.tif
- FigureS2.tif
- FigureS3.tif
- FigureS4.tif
- FigureS5.tif
- FigureS6.tif
- FigureS7.tif
- SupplementalTableS1.xlsx
- SupplementalTableS2.xlsx
- Supplementaryfigurelegends.docx